



## Characteristics of braking saccades in congenital nystagmus

Jonathan B. Jacobs<sup>1,3</sup>, Louis F. Dell'Osso<sup>1,3</sup> & R. John Leigh<sup>1,4</sup>

<sup>1</sup>Ocular Motor Neurophysiology Laboratory and <sup>4</sup>Neurology Service, Veterans Affairs Medical Center; and Departments of <sup>2</sup>Neurology and <sup>3</sup>Biomedical Engineering, Case Western Reserve University and University Hospitals of Cleveland, Cleveland, OH, USA

Accepted 15 November 2002

**Key words:** braking saccades, congenital nystagmus, saccade characteristics

### Abstract

Several of the characteristic waveforms of congenital nystagmus (CN) contain braking saccades. We test the hypothesis that braking (including foveating) saccades, while not always satisfying the standard relationships for saccades, are normal; any differences are due to the presence of high-velocity, slow-phase eye movements. Better measurements of saccadic properties, including position- and velocity-based measures and skewness, can eliminate some of this apparent distortion. We also evoked an analogous effect in normal subjects by use of a ramp-step-ramp stimulus. Finally, we used a model to further demonstrate this distortion in the saccades of normals, deviating from their intended magnitude as a function of the magnitude of the opposing velocity. The saccadic analysis methods developed herein are applicable to all saccades made during ongoing eye movements, whether normal or pathological. The above findings support the hypothesis that the braking saccades integral to many CN waveforms have normal characteristics and are the result of a normal saccadic system's responses to a slow-eye-movement oscillation.

**Abbreviations:** BDJ – bidirectional jerk; CN – congenital nystagmus; PC – pseudocycloid; PJ – pseudojerk; PP – pseudopendular; PP<sub>fs</sub> – pseudopendular with foveating saccades; PV – peak velocity; RSR – ramp-step-ramp; T – triangular; VOR – vestibuloocular response.

### Introduction

For over 25 years, a standard set of relationships has been used to relate the magnitude of a saccade to its duration and peak velocity (PV) [1–4]. Although the relationship is generally good, there is a scarcity of data for small saccades ( $<1^\circ$ ), and the different studies do not fully agree with one another. Saccadic relationships vary from person to person, and can even vary within the same subject [3].

Saccades can also fail to follow these standard relationships for a variety of reasons, including, but not limited to: ingestion of alcohol or other drugs [5]; neurological diseases such as Huntington's chorea or spinocerebellar degeneration [6]; or even the normal aging process [7–9]. These saccades generally have a lower PV and greater duration, although it is possible to encounter saccades that appear faster and shorter,

as in myasthenia gravis [10–12]. It has also been shown that saccades elicited under different conditions (e.g., visual versus non-visual) conditions can have slightly different properties, with visually evoked saccades being somewhat faster and shorter in duration than saccades made to remembered targets [13–15] or those made during antisaccade paradigms [16]. These differences may be attributed, in part at least, to the effects of higher cortical processing. Also, saccade magnitude can be diminished when combined with vergence movements [17].

In previous work [18, 19] we examined *braking saccades* [20] – small, stereotyped, fast eye movements that act to oppose (i.e., brake) the large slow-phase velocities (often in the range of 40–50°/s or greater) seen in congenital nystagmus (CN), some of whose oscillations probably originate in the smooth pursuit system [21–24]. In general, braking-saccade

magnitudes are not determined by visual information; however, they can be visually guided, in which case they are called *foveating* saccades, for they serve to foveate the target, as seen in, e.g., the jerk waveform of CN. The latter have been shown to be generated by the same pathways responsible for the programming of other visually guided saccades [25]. Braking saccades appear in several waveforms, including pseudopendular (PP), pseudopendular with foveating saccades (PP<sub>fs</sub>), pseudocycloid (PC), bidirectional jerk (BDJ), triangular (T) and pseudojerk (PJ) [26]. During our initial analysis of these saccades, we discovered that they did not always fit the standard relationships [18, 27], and for some subjects could appear slower than ‘normal’. Indeed, it has been claimed that the saccades in CN are slower than normal and a model was proposed for CN with that as its basis [28, 29]. This caused us some concern, for nonstandard saccades can suggest the possibility of pathology, yet all the data came from subjects with idiopathic CN: who had no known neurological deficits; whose ability to make accurate refixations to different targets is well-documented; and, more importantly, whose CN waveforms stem from a primary sinusoidal oscillation containing no saccades (i.e., the oscillation does not require a saccade for either its initiation or maintenance) [23, 24].

We hypothesize that braking saccades (including foveating saccades) are, in fact, normal saccades and that when they do not fit the standard relationships it is simply because they occur in the presence of, and act to oppose, CN’s high slow-phase velocities that tend to confound the accurate measurement of braking-saccade properties. We examined the techniques and assumptions usually made for the measurement of saccades, paying particular attention to the question of when saccades can be said to begin and to end, based on both position and velocity information.

## Subjects and methods

### Subjects

Data for this study came from seven CN subjects, five recorded explicitly for this study and two previously recorded in this laboratory, as well as four normal subjects who participated in the complementary ramp-step-ramp paradigm (discussed at the end of this section). Subjects are summarized in Table 1. All CN subjects had idiopathic CN without any ac-

Table 1.

	Subject	Sex	Age	Waveform	Number of saccades	Method
CN	1	M	33	PC*	116	IR
	2	F	49	PP <sub>fs</sub> —BS	66	IR
	3	F	14	PC	139	IR
	4	F	25	PC	214	Coil
				PP <sub>fs</sub> —BS	146	IR
	5	M	43	PP <sub>fs</sub> —FS	118	IR
			58	PC	31	Coil
				PP <sub>fs</sub> —BS	126	IR
	6	M	28	PP <sub>fs</sub> —FS	126	IR
				PP <sub>fs</sub> —BS	44	IR
	7	M	13	PC	42	IR
				Total: 1168		
Normal	8	F	47	RSR	178	IR
	9	M	40	RSR	187	IR
	10	F	33	RSR	168	IR
	11	M	28	RSR	180	IR
					Total: 713	

\* PC waveforms have only braking saccades. PP<sub>fs</sub> — pseudopendular with foveating saccades; PC — pseudocycloid; BS — braking saccades; FS — foveating saccades; RSR — ramp-step-ramp paradigm.

quired nystagmus and all subjects were healthy, with no neurological deficits. The CN subjects’ waveforms included either PP<sub>fs</sub> or PC cycles, and two subjects (S5 and S7) contained both. In primary gaze, S5’s waveform was usually PP<sub>fs</sub>, with PC occurring only at extreme gaze angles (40° left gaze). S7’s CN was mainly PC in primary gaze, with occasional intervals of PP<sub>fs</sub>. S7 had not been recorded extensively at other gaze angles, and consequently only the data for straight-ahead viewing were used. S2 and S6’s waveforms contained predominantly PP<sub>fs</sub> cycles, whereas S1, S3 and S4 displayed predominantly PC cycles. Records were chosen for study only if they contained repeated runs of braking saccades, to avoid using transitional cycles. When selecting PC cycles, care was taken to properly differentiate them from jerk with extended foveation, a similar-appearing waveform. If the distance from the apparent end of the saccade and the point of foveation was under 0.5° (for well-developed foveation, i.e., the ability to acquire the target in a *reliable* and *repeatable* manner with a minimal positional ‘jitter’, or spread of ±0.5°), the saccade was considered ‘foveating’ rather than braking, and the cycle was discarded. For subjects with

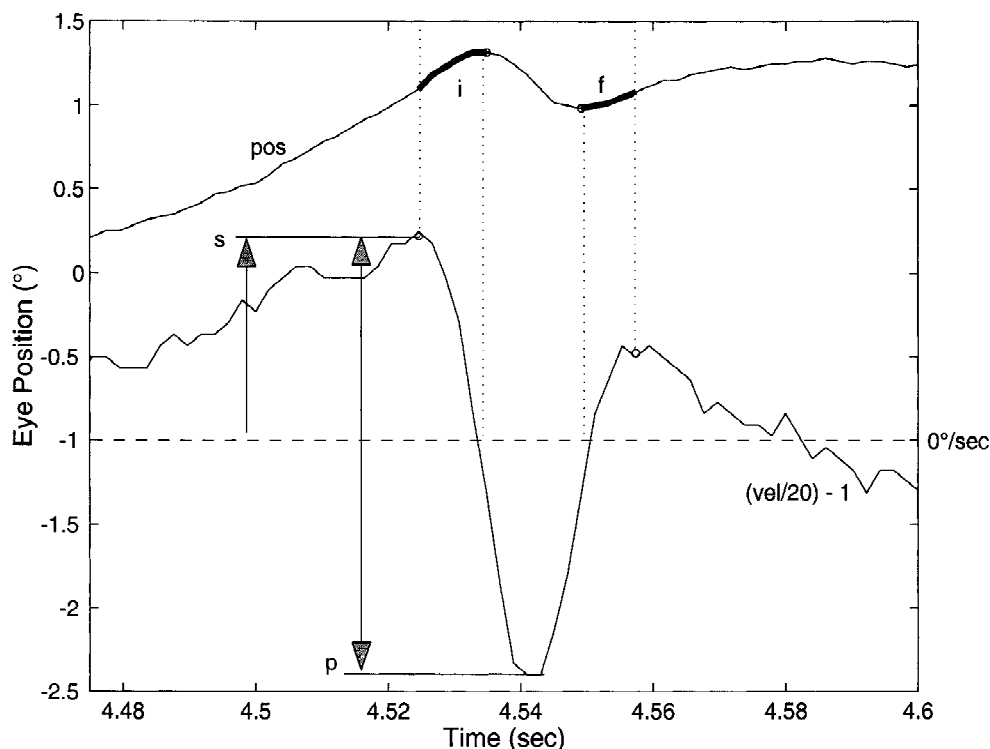


Figure 1. A schematic representation of the determination and differences between points of saccadic onset and offset. Top trace shows position, bottom shows velocity (divided by 20 and shifted vertically for clarity). The outer two dotted vertical lines represent the beginning- and end-points of the saccade as determined by the velocity data. Note that these points occur respectively earlier and later than their position-derived points. The single-headed arrow shows the value of slow-phase velocity ('s') preceding the saccade, the apparent PV is 'p', and the double-headed arrow shows the proper peak-velocity measurement, including the velocity of the preceding slow phase (p + s). The heavy segment, 'i,' on the position trace is the distance the eye traveled between the times of the velocity- and position-derived saccade onsets. Similarly, the segment 'f' is the distance traveled between the times of the position- and velocity-derived saccade offsets.

poor foveation, this criterion would have to be relaxed, as is done in determining the foveation window for the expanded nystagmus acuity function [30]. By using both  $PP_{fs}$  and PC waveforms from two of the subjects, we were able to perform an internal crosscheck, comparing our results both across subjects as well as across the waveforms for each subject. For S5 and S6's  $PP_{fs}$  waveforms, we also analyzed foveating saccades for comparison with the more simple braking saccades.

### Recording

Some horizontal eye movement recordings (subjects 1-3, 6-11) were made using infrared reflection (Applied Scientific Laboratories, Waltham, MA). In the horizontal plane, the system was linear to  $\pm 20^\circ$  and monotonic to  $\pm 25-30^\circ$  with a sensitivity of better than  $0.25^\circ$ . The IR signal from each eye was calibrated with the other eye behind cover to obtain accurate position

information and to document small tropias and phorias hidden by the nystagmus. Eye positions and velocities (obtained by analog differentiation of the position channels) were displayed on a strip chart recording system (Beckman Type R612 Dynograph). The total system bandwidth (position and velocity) was 0-100 Hz. The remaining data (subjects 4, 5) were recorded by means of a phase-detecting revolving magnetic field technique. The sensor coils consisted of nine turns of fine copper wire imbedded in an annulus of silicone rubber molded to adhere to the eye by suction. The system's sensitivity was less than one minute of arc, with linearity of one part in 14 014 and drift of 0.2-0.3 minarc/h. Noise was less than 2 minarc and eye position was stored to the nearest minarc [31]. The data were digitized at 500 Hz (with one subject recorded at 400 Hz, and one subject recorded on two separate occasions, once at 488 Hz and once at 500 Hz) with 16- or 12-bit resolution.

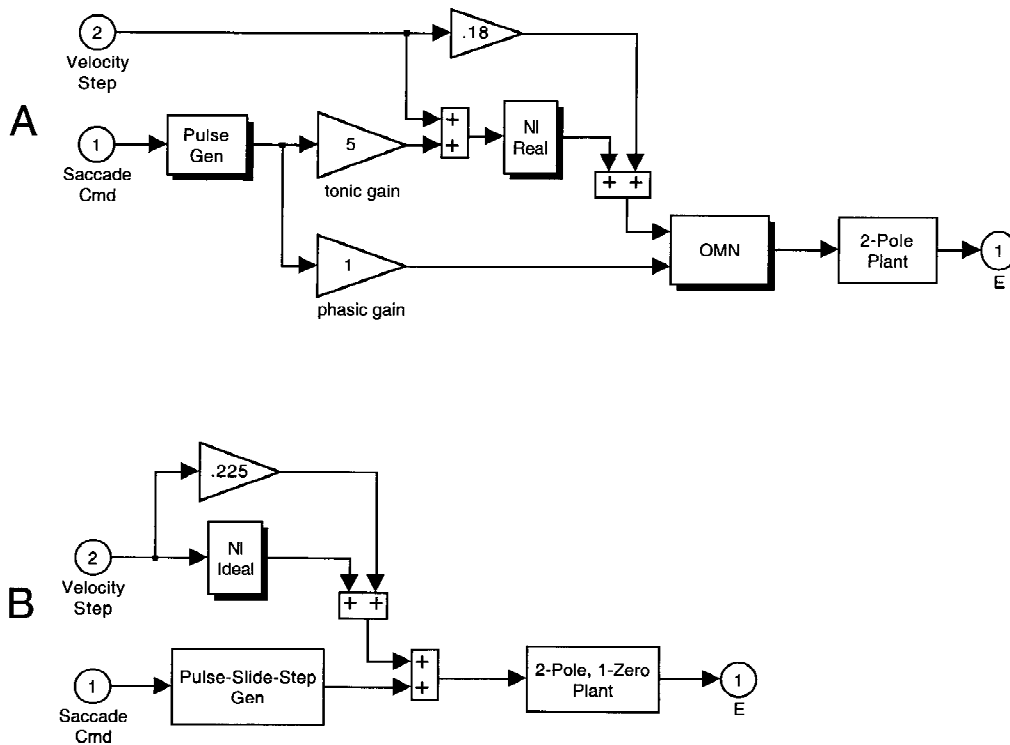


Figure 2. Open-loop model used to test the interaction between slow and fast phases. The pulse generator, neural integrator (NI), ocular motor neurons (OMN) and two-pole plant are taken from previous models. The two-pole, one-zero model comes from Zee et al. [44].

Recent findings [32, 33] indicate caution when using search coils in studies of saccade dynamics, as there can be decreases of approximately 5% of velocity leading to a concomitant increase in saccade duration. These effects appear to be due to alteration of the ocular motor signals by the act of insertion of the coil and, to our knowledge, has not been accounted for in previous studies. This may be the same mechanism that underlies the decrease in CN due to afferent stimulation, such as when the subject's forehead or trapezius is vibrated, or when they wear contact lenses [34], and that is implicated in the tenotomy of the extraocular muscles [35].

#### Protocol

Written consent was obtained from subjects before the testing. All test procedures were carefully explained to the subject before the experiment began, and were reinforced with verbal commands during the trials. Subjects were seated in a chair with headrest and either a bite board or a chin stabilizer, far enough (>5 feet) from an arc of red LEDs to reduce convergence effects. At this distance an LED subtended less than  $0.1^\circ$  of

visual angle. The room light could be adjusted from dim down to blackout to minimize extraneous visual stimuli. A CN experiment consisted of from one to 12 trials, including required *monocular* and *binocular* calibrations, each lasting up to 1 min with time allowed between trials for the subject to rest. Trials were kept short to guard against boredom because CN intensity is known to decrease with inattention. All trials were fixation trials with the subject kept stationary; no pursuit or vestibuloocular responses (VOR) were involved.

Ramp-step-ramp (RSR) experiments were performed monocularly and consisted of eight trials of up to 75 s of a random series of constant-velocity ramps of 10, 20, and  $40^\circ/\text{s}$  interrupted in the center by a step (of 1, 5, or  $10^\circ$ ) that was either in the same direction as the ramp or in opposition ('with' and 'against' cases). The step was then followed by the resumption of pursuit at the same velocity. Each subject was presented with three of every possible combination of ramp and step. Prior to the pursuit trials, the subjects were presented with two series of target jumps of the same magnitude as the steps, but without the pursuit ramp, to provide a baseline for saccadic parameters.

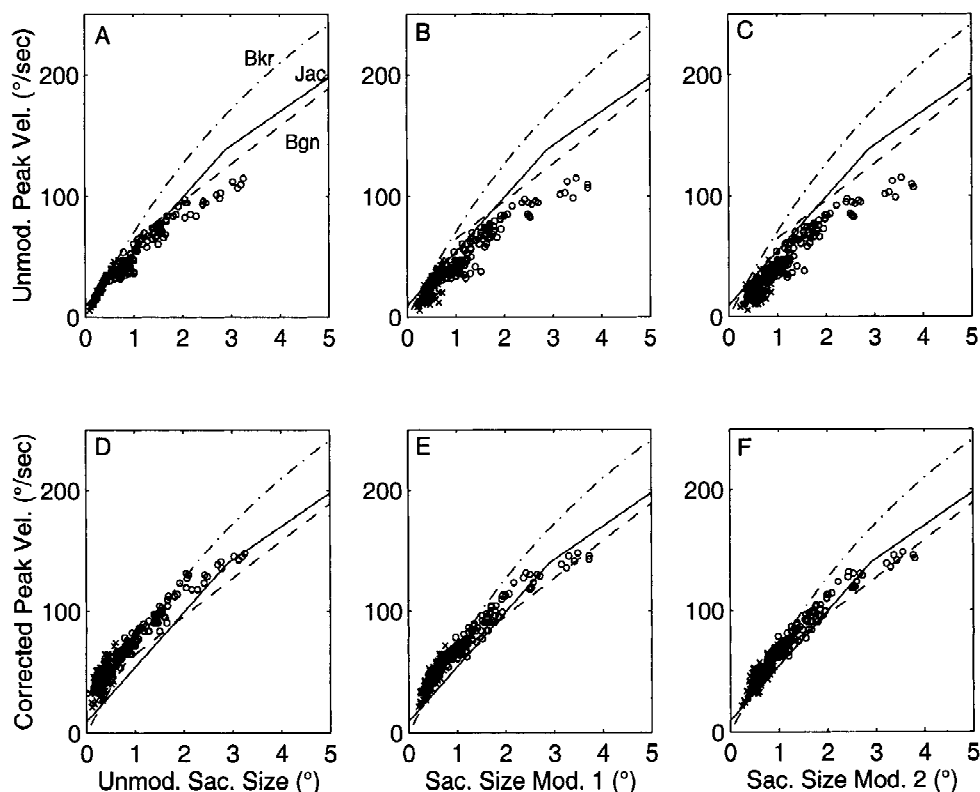


Figure 3. Peak velocity versus amplitude for the braking and foveating saccades in S5's  $PP_{fs}$  waveform. Panels A–F show the six calculated possible corrections based on three ways of adjusting the magnitude and two ways of measuring PV. In this and Figures 4–6, top row (A–C) is uncorrected PV, and bottom row (D–F) is corrected PV. First column (A, D) is unmodified saccade magnitude; second column (B, E) adds the initial saccadic segment; third column (C, F) adds initial and terminal saccadic segments as discussed in the text. In this and Figures 4 and 10, curve 'Bkr' comes from Becker, curve 'Bgn' comes from Boghen et al., representing mean PV (high and low limits for 95% of measured saccades start at  $5^\circ$  – beyond the range of these data – and therefore are not shown), and curve 'Jac' was fit to the 350 baseline saccades made by the normal subjects in this study. In this and Figures 5 and 7, braking saccades = 'x'; foveating saccades = 'o' Note that lower range of foveating saccades and upper range of braking saccades overlap.

### Analysis

All analysis was carried out in the MATLAB environment (The MathWorks, Natick, MA) using software written for this study. Only eye position was sampled directly, with velocity derived from the position data by means of a variable degree central-point differentiator. This common method estimates instantaneous velocity by taking the difference between a point  $n$  samples prior to the current sample point and a point  $n$  samples after the current sample point (a process applied to the data *post hoc*), and dividing the result by the interval between the points. The central-point differentiator is equivalent to an ideal differentiator followed by a low-pass filter. As  $n$  increases, the cutoff frequency decreases and the effective low-pass filtering increases accordingly. The data in this study

(normal and CN) were filtered with  $n = 2$ , resulting in peak velocities  $\geq 94\%$  (for 488- and 500-Hz data) and  $\geq 90\%$  (for the one subject with 400-Hz data) of their minimally filtered values (i.e., differentiated with  $n = 0$ ). According to mathematical theory, the 3-dB bandwidth for data sampled at 500 Hz, filtered with  $n = 2$  is 55.37 Hz [36], so the attenuation could be as great as 10% for signal frequencies around 30 Hz. Fortunately, spectral analysis of our small-saccades data show that the bulk of the signal energy is concentrated *below* this point. Furthermore, explicit checks of the *actual* attenuation were performed by comparing the filtered ( $n = 2$ ) and minimally filtered ( $n = 0$ ) peak velocities of more than 75 saccades randomly selected from five of the subjects, yielding less than a 10% difference. Finally, and most importantly, any effects of differentiation and filtering on the peak velocities of the

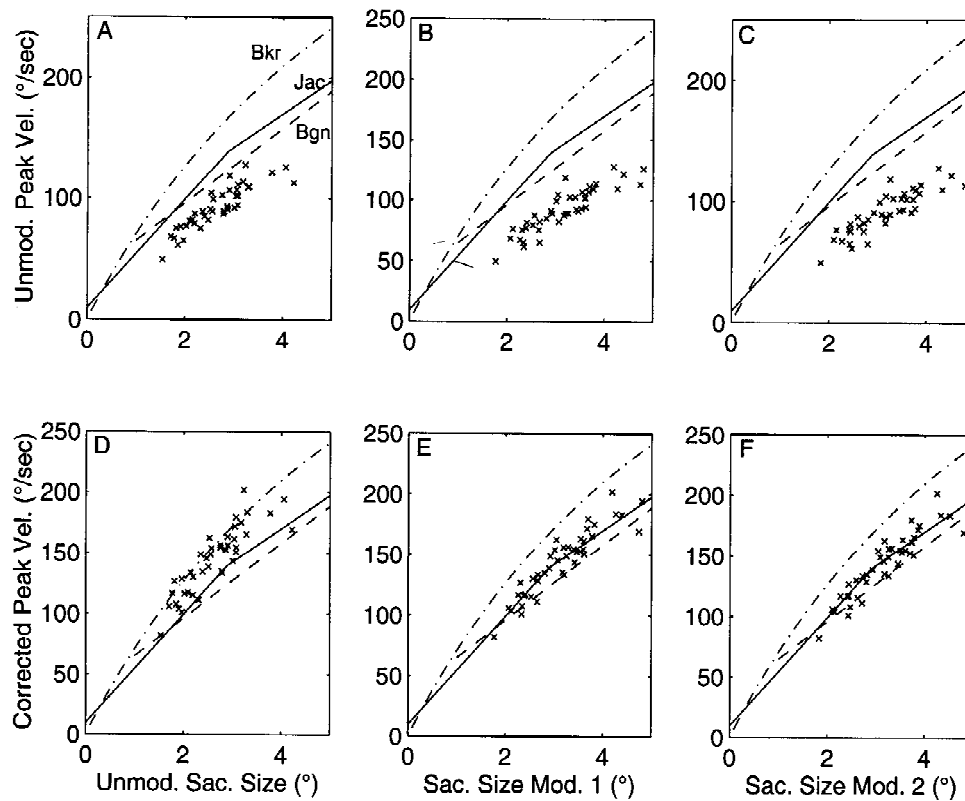


Figure 4. Peak velocity versus amplitude for the braking saccades in S7's PC waveform. Panels A–F show the six calculated possible corrections based on three ways of adjusting the magnitude and two ways to measure PV.

saccades examined *applied equally* to both the braking and foveating saccades from our nystagmus subjects as well as to the baseline saccades and RSR saccades made by our normal subjects. The importance of this consistency can be seen because comparisons of our peak-velocity data for the baseline saccades of the normal control subjects using this differentiator match those in the literature (filtered in a variety of manners), including the data for small saccades with amplitudes in the range of braking saccades. Others have claimed minimal effects using a Butterworth filter [37], and it has also been found that a central differentiator could actually *increase* the PV estimate [38]. Based on these observations, we believe that concerns about diminishment of PV that has been ascribed to filtering [36], do not apply, given the methods we employed.

#### Saccade duration

To calculate the properties of a braking saccade, we are interested in its beginning, its end, and the point at which the maximum velocity is reached. However, these measures are not as straightforward as one might

hope, because braking saccades are made in the presence of a high-velocity, accelerating slow phase that has a confounding effect on them. When examining the position record, the first inclination might be to state that the beginning of the saccade occurs when the eye position reaches a local maximum (or minimum) and then reverses itself (Figure 1). Similarly, we might consider the end of the saccade to be the time when the eye resumes its movement in the opposite direction. If not for the presence of the CN oscillation and its associated velocity, this would be a reasonable approach. This can be seen by examining the velocity record. The beginning of a saccade made in the presence of a non-negligible slow-phase velocity can be determined in the same manner as that of a saccade when the slow-phase velocity is zero, or nearly so. The beginning and end of the saccade are the points at which the velocity reverses (Figure 1). This differs from the usual method (used later for saccadic outputs from the model), where the first point that exceeds a threshold baseline velocity (e.g., 5°/s) is considered the point of onset. This is because in CN there is no

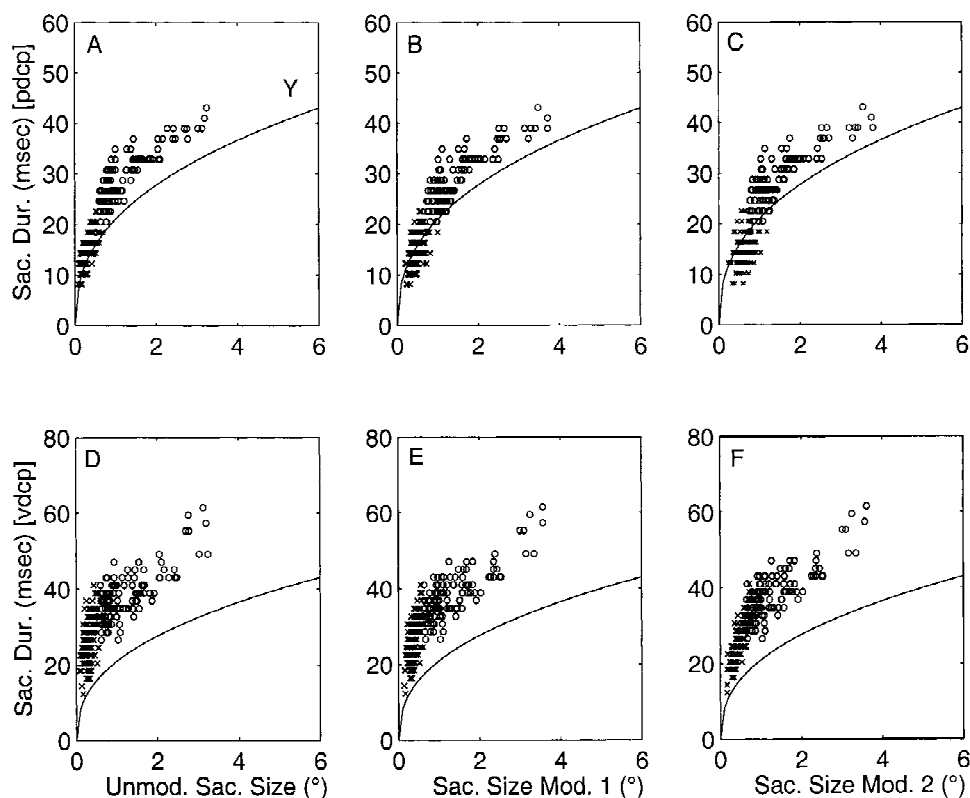


Figure 5. Duration versus amplitude for the braking and foveating saccades in S5's  $PP_{fs}$  waveform. Panels A–F show the six calculated possible corrections based on three ways of adjusting the magnitude and two ways to measure duration. In this and Figure 6, curve 'Y' comes from Yarbus. Note that lower range of foveating saccades and upper range of braking saccades overlap.

reliable velocity baseline, as the slow-phase velocity is accelerating. The difference between these two methods is quite minor, fortunately, generally just a sample point, leading to potential errors of  $\pm 2$  ms (at 500 Hz) at either end, or  $\pm 4$  ms overall.

We manually selected saccadic onset and offset using both the position and velocity records. However, comparison of these onset/offset pairs will show that the saccadic onset derived from the position record does not correspond with the onset derived from the velocity record; nor do the offsets. The velocity-derived onset occurs several samples before the position-derived onset, while the velocity-derived offset occurs after the position-derived offset. Specifically, the position-derived points occur within the interval marked by the velocity-derived points (Figure 1) (even after allowing for the properties of the central difference estimator, by subtracting the time shift at each end due to differentiation; for  $n = 2$  we moved the v-onset and -offset points inwards two samples), approximately at the zero-crossings of the

saccadic velocity record, as would be expected since the position-derived offsets mark the points where the eye has changed direction and, therefore, briefly has no velocity. Comparison of the onset/offset points with differentiation of  $n = 3$ ,  $n = 2$  and  $n = 1$  showed little systematic variation; they were about as likely to shift (usually by a single sample) in either direction depending on the magnitude and frequency characteristics of any noise in the signal and were frequently not affected at all. This jitter was also observed when examining saccades made by our normal subjects, when viewing both static and ramp-step-ramp targets, so it is not an artifact of the non-zero, slow-phase velocity.

We considered the use of acceleration-derived onset/offset points in the hope that they would help us further segregate the effects of the slow-phase velocity from the saccade dynamics. However, even after filtering, the acceleration signal was too noisy to allow reliable identification of onset/offset points in any consistent fashion. This often added an extra level of uncertainty on the order of  $\pm 2$ –3 samples for each

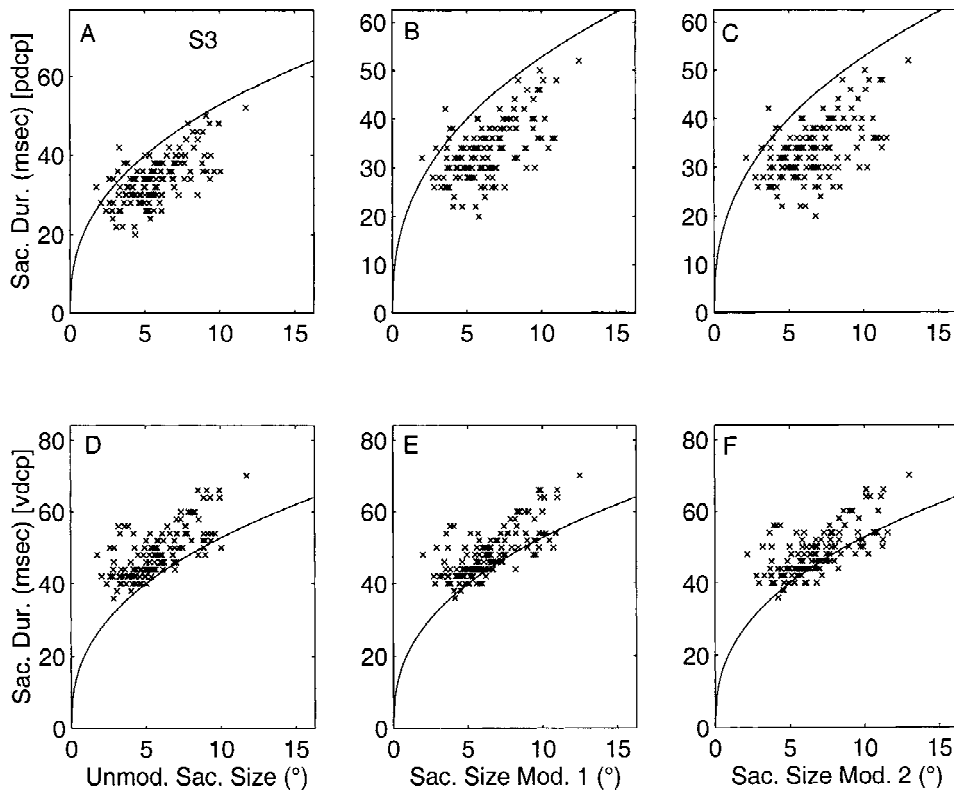


Figure 6. Duration versus amplitude for the braking saccades in S3's PC waveform. Panels A–F show the results after applying the possible corrections.

point, which in some cases could coincide with the timing of the velocity-derived points, but potentially resulted in less reliability.

#### *Saccade peak velocity*

When measuring the PV of a braking saccade, once again the velocity of the slow phase must be accounted for. Simply measuring the peak of the velocity record is not sufficient, the slow-phase velocity at the beginning of the saccade must be added. This is also illustrated in Figure 1. To count only the velocity from zero to the peak ('p') ignores a major portion of the saccade (the segments that occur before the first zero crossing, and after the second zero crossing) and therefore leads to a false, low value for the velocity. Winters et al. recognized this when they studied normal saccades in the presence of high-velocity VOR [39]. Therefore, we started the measurement from this shifted baseline, adding the magnitude of the initial slow-phase velocity ('s') to obtain a more accurate measurement of PV (indicated by the double-headed arrow).

We also examined the result of making a linear interpolation between the velocity-derived saccadic onset and offset times and adding the velocity 'p' to that intermediate velocity. There was no qualitative difference in the resulting plots of corrected PV versus saccade magnitude; the difference between the velocity at this intermediate time and the beginning of the saccade (the time we are using) ends up, in general, being a small part of the total corrected velocity, for the smaller saccades that constitute the bulk of our data, e.g., about 10–15% for the braking saccades in the PP<sub>fs</sub> waveforms, although it could be up to 20% in some subjects' PC cycles. We fit sine curves to the slow phase velocity (to mimic the underlying pendular CN) and verified that subtracting the slow-phase from the saccade did not affect the timing of the PV for either large (5°) or small (<1°) saccades. Therefore the skewness calculations were also unaffected.

#### *Saccade magnitude*

We considered several methods of calculating the magnitude of a braking saccade. The first, and easiest,

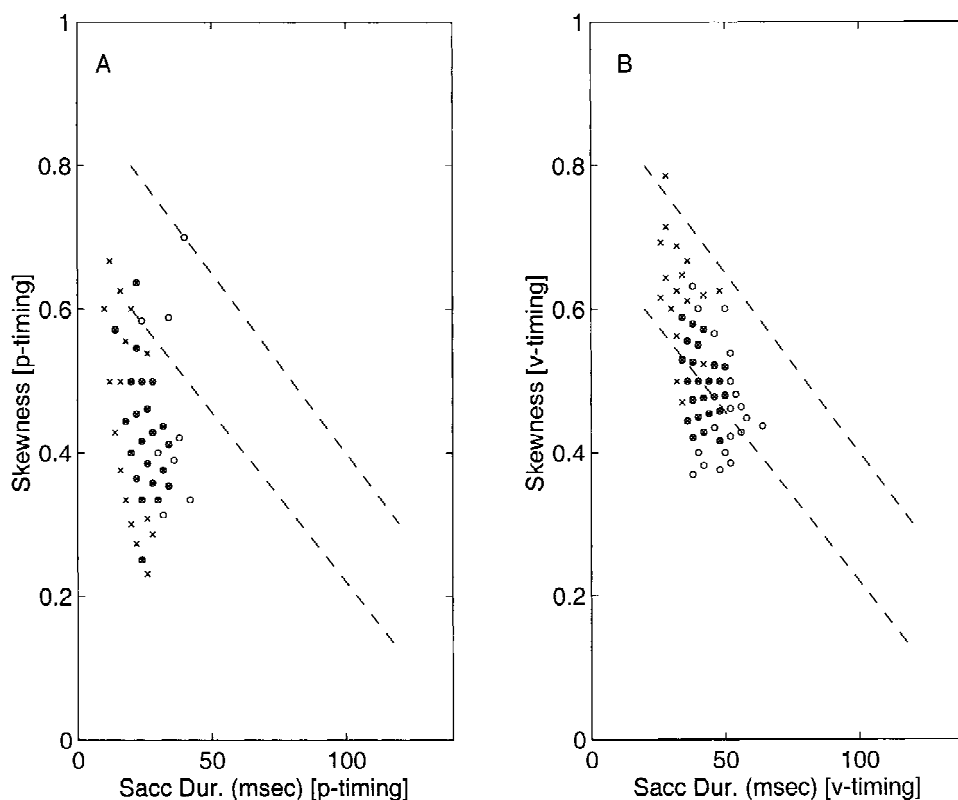


Figure 7. Skewness versus duration for the braking and foveating saccades in S6's  $PP_{fs}$  waveform. (A) Using velocity-derived onset and offset points. (B) Using position-derived onset and offset points. Dashed lines represent upper and lower bounds of skewness from van Opstal and van Gisbergen.

is simply to use the position-derived onset and offset points, and calculate the difference in position at these times. The problem with this standard approach (used for normal saccades between stationary targets) is that it leads to artificially reduced measures of amplitude, for it does not take into account that the eye was moving with great velocity in the other direction due to the CN and therefore took some amount of time to slow and reverse.

These considerations lead to two possible approximations that may be used to better determine 'true' (i.e., the intended) saccadic size. For the first modification to saccade size, we simply added the distance the eye traveled between the time the velocity-derived saccade onset occurred and the time the position-derived onset occurred (labeled 'i' in Figure 1) to the magnitude obtained by using only the position-derived onset and offset. For the second modification we also added the distance traveled in the time between the position-derived and the velocity-derived offsets (labeled 'f'). The diminishment of the saccade is essentially equal to the opposing slow-phase velocity

multiplied by the 'i' and 'f' durations which are difficult to calculate explicitly for CN, as the velocities are not constant but may be changing exponentially. This makes the direct measurement of the 'i' and 'f' magnitudes a good first-order approximation but might cause a slight over-correction. Although the initial acceleration builds rapidly in the first few milliseconds, the eye must overcome its inertia, and changes position slightly. However, our examination of the baseline saccades made by our four normal subjects, in the first 6 ms of a  $5^\circ$  saccade, revealed that, at most, the eye traveled between  $0.1$  and  $0.15^\circ$ ; the distance traveled in the terminal portion was similarly small. We adopted this approach as an attempt to 'bracket' the possible range of corrections, using an over-estimation at the high end, and no correction at the low end. Adding only the 'i' (or the 'f') component provides an intermediate state between no correction and full correction.

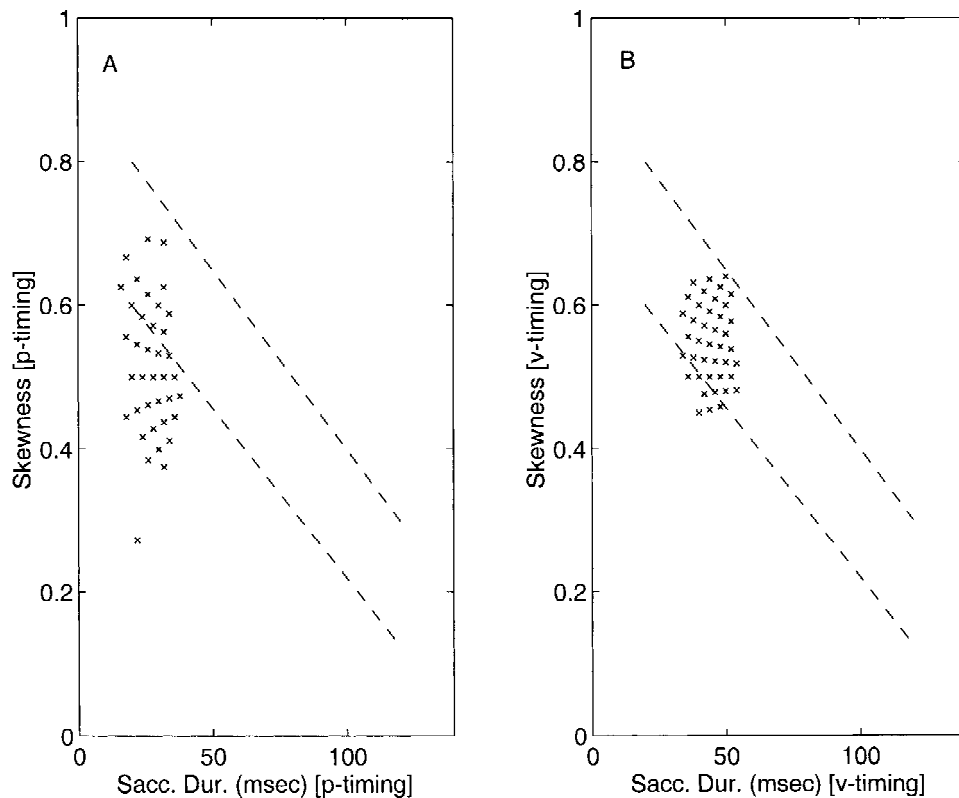


Figure 8. Skewness versus duration for the braking saccades in S4's PC waveform. (A) using velocity-derived onset and offset points. (B) using position-derived onset and offset points.

### Saccade skewness

Skewness is a measure of the symmetry of a saccade's velocity profile, i.e., acceleration and deceleration. It provides more information about saccade dynamics than is available in the three standard parameters. Smaller saccades appear more symmetric (i.e., their accelerating and decelerating phases are roughly equal), whereas larger saccades tend to accelerate to their PV quickly and then 'coast' the rest of the way, yielding a skewness below 0.5 [40, 41].

There are several methods to calculate skewness; some of them are quite mathematically intense, requiring the use of gamma functions [14], or the computation of higher order central moments. Fortunately, all give similar results so we used the simplest one, the ratio between the time to PV of the saccade and its duration [40]. A symmetrical saccade therefore has a skewness of 0.5; one that is slow to accelerate to PV,  $>0.5$ ; and the skewness of one with a long decelerating 'tail' is  $<0.5$ . Because skewness depends on saccade duration, we compared skewness results

calculated by use of position- and velocity-derived saccadic onsets and offsets.

### Foveating saccades

The above analyses were also performed for foveating saccades from S5 and S6's  $PP_{fs}$  waveform (PC waveforms do not have a foveating saccade; the braking saccade starts the eye towards the target and a slow eye movement brings it to the target).

### Ramp-step-ramp

Saccades made by the normal subjects were subjected to the same analyses of PV, duration, and skewness as those made by the CN subjects. Results of the saccades made either with or against pursuit ramps of different velocities were compared to those made when no initial velocity was present.

### Models

We constructed two simplified, open-loop control system models of the saccadic system in the MATLAB/Simulink environment, consisting of a pulse

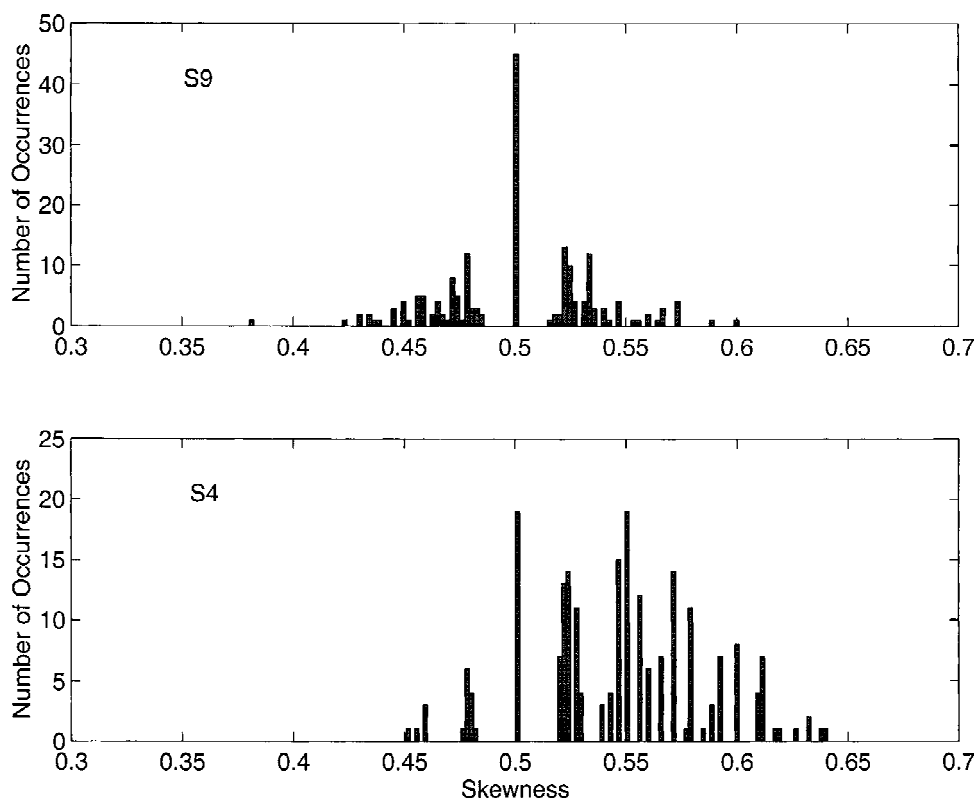


Figure 9. Histogram of the distribution of saccadic skewness for S9, a normal subject (top panel), and the braking saccades from S4, a CN subject with a PC waveform (bottom panel). The normal subject is more symmetrically and sharply distributed around 0.5.

generator, neural integrator, ocular motor neurons and plant (Figure 2A,B). The first model used components from our previous models of both congenital and latent nystagmus [23, 42, 43], creating a pulse-step to drive a two-pole plant with time constants of 7 and 180 ms. The second model, which used a pulse-slide-step to drive a two-pole, one-zero plant (zero at 80 ms, real poles at 300 and 13 ms, and a pair of complex poles), came from Zee et al. [44], with modifications to allow symmetric operation without being connected in push-pull.

Both models had two independent inputs, a saccadic command and a pursuit (velocity step) command, that were combined linearly to simulate a first-order approximation of the interaction between the slow- and fast-phase subsystems. We first verified that these models could make accurate saccades in the absence of an initial velocity. We then generated saccades of specific intended magnitudes in the presence of a variety of constant velocities, as great as 50°/s, comparable to the slow-phase velocities typical of CN. Ramps and saccades were combined in both the ‘with’ (ramp facilitating saccade) and ‘against’

(ramp opposing saccade) directions. We measured the resulting saccades, comparing them to their intended magnitudes and durations.

## Results

### *Peak velocity versus amplitude*

Figure 3A–F shows the results for PV plotted versus magnitude for S5’s PP<sub>fs</sub> waveform for both braking (‘x’) and foveating (‘o’) saccades. The braking saccades are quite small, frequently under 1°, and the foveating saccades range from approximately 1° to just under 4°. There is a small amount of overlap between the upper range of braking saccades and the lower range of the foveating saccades. There are six subplots displayed, representing the possible combinations resulting from two methods of measuring PV and three methods of measuring amplitude. Panels A–C show peak-velocity calculations that do not account for the initial slow-phase velocity; D–F are recalculated to include this velocity. In panels A and

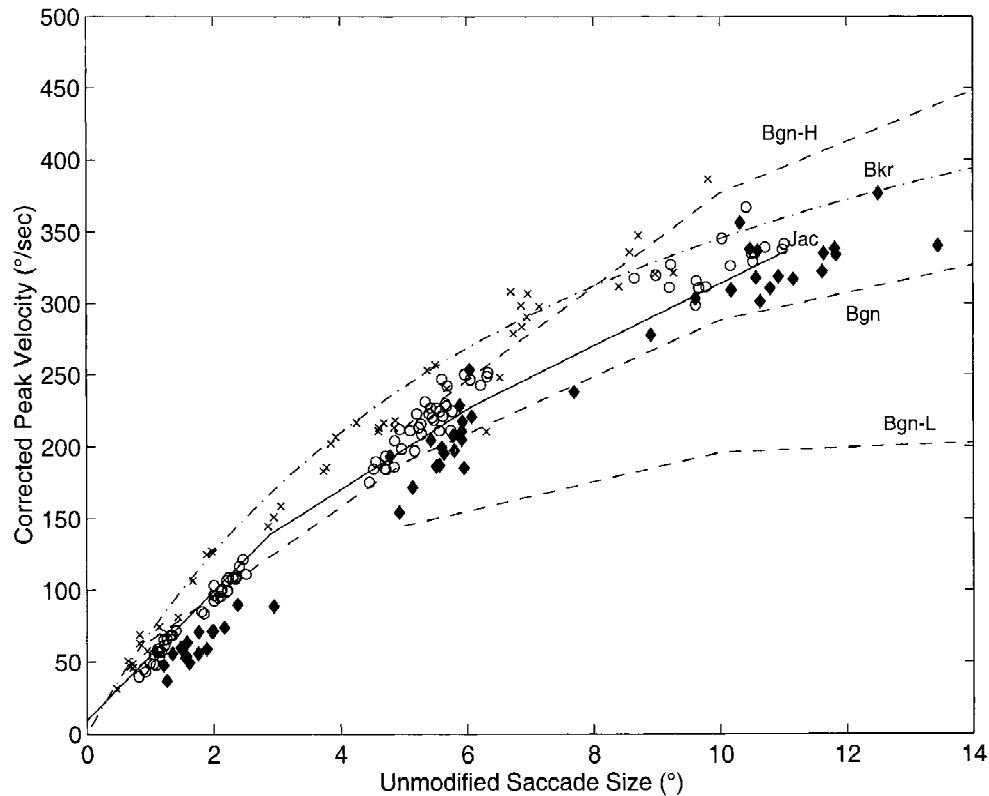


Figure 10. Ramp-step-ramp PV versus amplitude results for saccades from normal subject S9. Saccades made in the absence of smooth pursuit (i.e., normal saccades) = 'o'; against smooth pursuit = 'x,' with smooth pursuit = 'diamond.' Curve labels are as in Figures 3 and 4.

D the saccadic magnitudes are recorded using only the position-derived onset and offset points. Panels B and E incorporate the addition of the distance the eye traveled between the velocity- and position-derived onsets. Finally, Panels C and F include the onset correction in addition to the distance traveled between the position- and velocity-derived offset times. The same criteria were used to calculate the data in each panel in Figures 4–6. The curve marked 'Bkr' is the PV versus amplitude relationship from Becker [45], and the curve marked 'Bgn' is from Boghen et al. [3]; both are representative of prior saccadic parameter studies. The difference in the mean curves possibly reflects methodological differences. The 95% intervals for the fastest and slowest peak velocities are not displayed here, as they begin at 5°, which is beyond the upper end of these saccades. We also calculated a piecewise-linear fit to the baseline saccades made by the normal subjects (four subjects, 350 saccades, ranging from 1° to 10°, made in the absence of any slow-phase velocity); for saccades from just over 0.4° to 3°, the slope is  $44.87 \text{ s}^{-1}$ , with a  $y$ -intercept of  $9.537^\circ$ , and an  $r^2$  value of 0.928. This curve, marked 'Jac,' is shown in

Figures 3 and 4, for comparison with the relationships calculated by Becker and by Boghen.

In the top three panels (A–C), when we do *not* include the slow-phase velocity in the calculation of PV, all the saccades appear to be somewhat slow, albeit within the 'acceptable' range. As we apply the magnitude corrections, to include more of the saccade that had been masked by the runaway slow phase, the fit worsens as the points shift towards higher magnitudes.

The bottom three panels (D–F), show the opposite result; now that the entire change in velocity is included in the measurement of PV, the saccades are shifted so that they appear to be slightly faster than average. As components 'i' and 'f' are included in the magnitude calculation, the points move closer to the curve, corresponding particularly well with the 'Jac' curve, i.e., the same area where our normal subjects' saccades lay. These results are similar to those obtained for S2's and S6's  $PP_{fs}$  braking and foveating saccades.

The results for PV versus magnitude for S7's PC waveform are plotted in Figure 4. These saccades are much larger than those seen in S5's  $PP_{fs}$  wave-

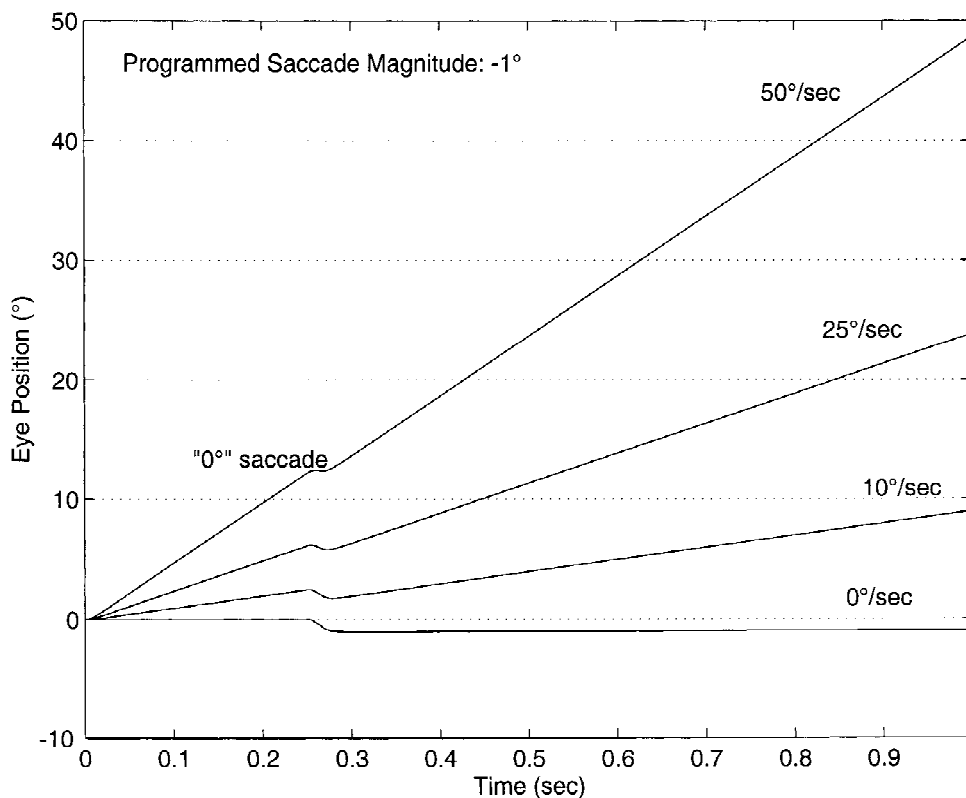


Figure 11. Examples of  $-1^\circ$  (intended magnitude) saccades made in the presence of smooth pursuit in the opposite direction for the two-pole model. Labeled outputs are shown for velocities ranging from  $0^\circ/s$  to  $50^\circ/s$ . Note the greatly diminished saccade in the  $50^\circ/s$  case; it is nearly a 'saccade of zero magnitude'.

form. As with S5, the saccades follow the general principle that PV increases with magnitude, regardless of measurement methodology. Once again, prior to the peak-velocity correction, saccades appear slow, and after the velocity correction they conform more closely to normal values, regardless of whether the magnitude correction is applied. Here, the fit to the 'Jac' curve is even better than in the previous figure. This figure illustrates the observation that we noted for approximately 50% of our subjects: the velocity correction alone results in peak velocities that exceed the average peak velocities of normals. In those cases, it is necessary to apply both the velocity and magnitude corrections (see Discussion). These data were typical of those subjects with PC waveforms.

#### *Duration versus amplitude*

Figure 5A–F shows the results for duration versus magnitude for S5's  $PP_{fs}$  waveform. As in Figure 3, both braking and foveating saccades are shown and there are six subplots in this figure, representing the

combinations of the two ways to measure duration and the three to measure magnitude. The solid curve represents the duration versus magnitude data from Yarbus [2]. The fit for the position-derived duration comes closer to the standard curves than does that for the velocity-derived duration due to this subject's propensity to make dynamic overshoots.

Duration versus magnitude results are plotted in Figure 6A–F for S3's PC waveform. In contrast to the case above, before the corrections are applied, these saccades appear to be of shorter duration than average; after correction, they are closer, albeit slightly larger, than average. Equivalent results were obtained for the remaining subjects. As expected, no matter what correction was attempted, the larger a saccade, the longer its duration. Thus, the duration, PV, and magnitude general relationships hold regardless of methodology.

#### *Skewness*

Figure 7 shows a plot of skewness versus duration for S6's  $PP_{fs}$  waveform, for both braking and foveat-

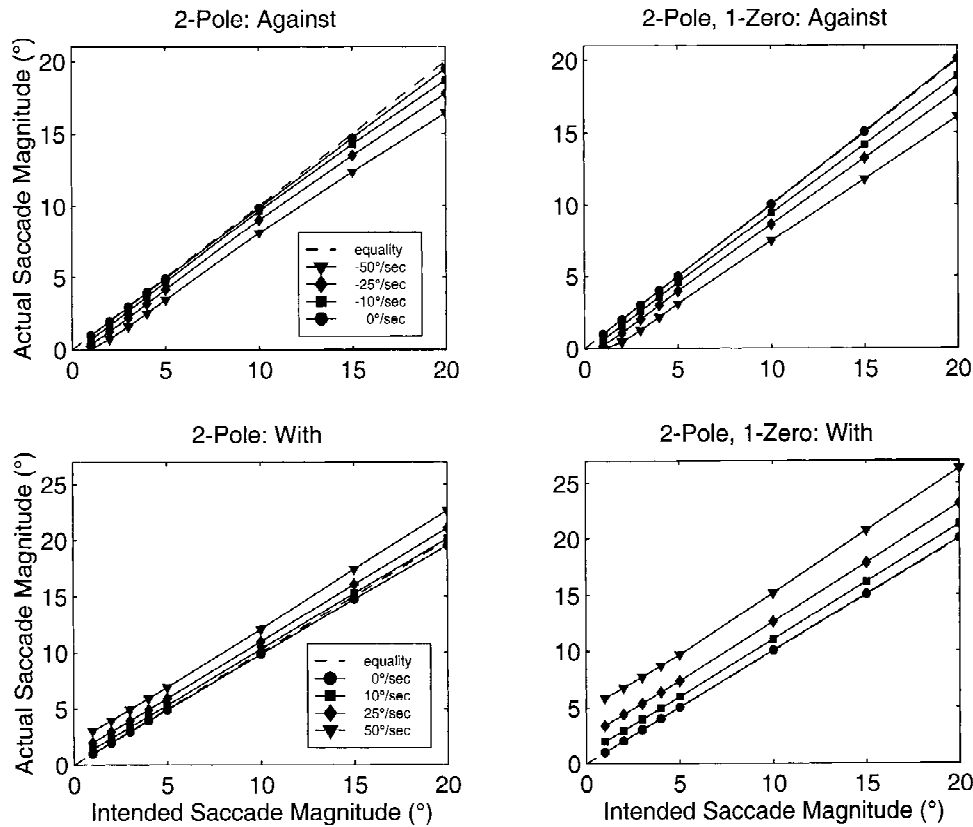


Figure 12. Relationships between inputs (intended saccades) and outputs (actual saccades) of the model, testing summation of slow phases with opposing fast phases. Left column shows response data of the two-pole model and right column, of the two-pole, one-zero model. Top row represents saccades made against the slow-phase velocity and bottom row, saccades made with the slow-phase velocity. Note that the two-pole model's larger saccades for a 0°/s slow phase are just below the dashed line of equality, due to real-life characteristics of the model's saccadic system.

ing saccades. The dashed lines are adapted from van Opstal and van Gisbergen [40] and show the approximate bounds of their results. Note that the upper range of the braking saccades ('x') overlaps well with the lower end of the foveating saccades. For the foveating saccades ('o'), the velocity-derived duration in plot 7B yields a better fit to reported results than do the position-derived durations seen in plot 7A, while the braking saccades do not show quite as much improvement. Analysis of other subjects' waveforms ( $PP_{fs}$  or PC) yielded similar results, as shown in Figure 8 for S4's PC braking saccades using velocity-derived durations. Again they offer much better correspondence than do the position-derived ones.

The skewness of S4's saccades, shown in the histogram in Figure 9, Bottom, using the velocity-derived durations, are distributed around 0.5, as would be expected for saccades that fall in this range (smaller than 5°). Compare this to the skewness distribution for all

saccades made by normal subject S9 (Figure 9, Top), showing a peak more strongly centered on 0.5 than the skewness of braking and foveating saccades made by the CN subjects, who as a group, tended to have a looser distribution around 0.5, possibly due to the difficulty in accurately determining the onset of saccades in the presence of high-velocity slow phases.

#### Ramp-step-ramp

Normal subject S9's performance at all pursuit velocities tested in the RSR paradigm is representative of the results seen in all the normal subjects, and is summarized in Figure 10 as a plot of PV versus magnitude for saccades made with no pursuit ('o'), saccades made against pursuit ramps ('x'), and saccades made in the same direction as pursuit ('diamond'). Note the distinct separation for these three cases, with saccades that must overcome the opposing pursuit having a

larger PV than static saccades, which in turn have a higher PV than those saccades that ‘ride along’ in the same direction as pursuit. The PV is corrected as described earlier, but the magnitude corrections have *not* been applied, so as to demonstrate the effect on apparent magnitude that an opposing or facilitating slow-phase can have.

At the higher pursuit velocities ( $\pm 20$  and/or  $\pm 40^\circ/\text{s}$ ) all the normal subjects frequently made catch-up saccades. Their properties were found to be indistinguishable from those of the RSR saccades and therefore were included in the analyses.

Examination of saccadic durations, however, reveals little if any change for saccades made during no pursuit; when pursuit was  $\pm 10^\circ/\text{s}$ , the velocity-derived timing tended to yield slightly longer saccades, frequently adding a sample point or more at each end. For pursuits of  $\pm 20^\circ/\text{s}$  and  $\pm 30^\circ/\text{s}$  the difference could be more noticeable, up to three sample points at either end. This was not an invariant result, however; it was possible for pursuit cases to show no change in duration between position- and velocity-derived points, and for slow pursuit to be several samples longer at either end. Also, these differences were seen regardless of whether the pursuit was in the same direction as the saccade or in opposition. The results presented here were based on the velocity criteria.

### Models

The interaction between initial smooth-pursuit velocities and resulting saccadic sizes is demonstrated by outputs from the two-pole model shown in Figure 11, for a  $1^\circ$ -programmed leftward saccade, combined with ramps ranging from 0 to  $50^\circ/\text{s}$  in the opposite direction. For lower velocities, the magnitude of the resulting saccade is only slightly affected, but at the highest velocity ( $50^\circ/\text{s}$ ), the cancellation is so severe that the saccade appears nearly flat, in effect a saccade of ‘zero magnitude’, a phenomenon we reported in previous work [19]. Equivalent results were obtained with the two-pole, one-zero model.

Figure 12 quantifies the relationships between intended and actual saccades produced by both models for three cases: (1) saccades with no additional slow-phase velocity; (2) saccades with a slow-phase in same direction as the saccades; and (3) saccades with an oppositely directed slow-phase velocity. The dashed line in all four panels is that of saccadic equality; i.e., points along this line are those whose intended and actual magnitudes are identical. Note that the two-

pole model’s output for no slow-phase velocity falls just below this line at the higher magnitudes ( $\geq 15^\circ$ ) while the two-pole, one-zero model’s output lies along the line. This is due to the design of the two-pole model’s saccade generator that attempts to realistically simulate the common human tendency to be slightly hypometric for larger saccades.

As predicted, when the initial velocity and the saccade are oppositely directed, the resulting saccade is smaller than its programmed value (the lines for  $-10^\circ/\text{s}$ ,  $-25^\circ/\text{s}$  and  $-50^\circ/\text{s}$ ). Conversely, when the initial velocity and the saccade are in the same direction, the resulting saccade is appreciably larger than it would have been in the absence of a pre-existing velocity, with the effect growing more pronounced as that velocity rises to  $50^\circ/\text{s}$ . The data in Figure 12 are for rightward saccades; the results for leftward saccades are identical.

The amount of diminution or enhancement depends on the programmed magnitude of the saccade, the initial velocity, and the characteristics of the plant. The two-pole, one-zero plant shows a greater effect when saccades and initial velocity are in the same direction and, to a lesser extent, when they are in opposition. When viewed as a percentage change, the effect is most pronounced for smaller saccades, and decreases as programmed saccade magnitude increases. The effect is also greater when the pursuit velocity increases, as expected.

Next, we measured the duration of the saccade, as determined by velocity criteria, for all combinations of saccade and initial-velocity magnitudes and directions using both models. In all cases the duration of a saccade of a given pre-programmed magnitude remained the same (within  $\pm 1$  sample onset and offset) regardless of the magnitude and direction of the slow-phase velocity.

Finally we attempted to ‘reconstitute’ the initially programmed saccade from the diminished saccade produced by the ‘against’ case, by the same method we employed to correct braking saccades. The resultant saccade ranged from 75 to 95% of the programmed magnitude, depending on the programmed magnitude and opposing velocity, with larger saccades coming the closest to full correction.

### Discussion

The goal of this study was to examine the characteristics of braking saccades and attempt to reconcile them

with the standard relationships used to characterize other types of fast eye movements. It had been hypothesized that the complex waveforms of CN were created by the responses of a normal saccadic system to an ongoing oscillation [23, 26]. Because braking saccades act to oppose the runaway slow-phase velocities of CN, there is some degree of interaction between the two motions. We have studied and modeled the simplest possible interaction, namely the simple linear increase and decrease of saccadic magnitudes, peak velocities, and durations due to the summation and cancellation of fast and slow phases at the plant.

We examined two reasonable approaches to correct saccadic magnitude, adding an approximation of the distance the eye traveled during the times between when position-derived and velocity-derived timing indicated the saccade occurred. It appears that the most appropriate metric is the velocity-derived saccadic duration; from this value it is then possible to work ‘backwards’ to approximate the magnitude of the programmed braking saccade. The methodology developed to study braking saccades is directly applicable to all saccades made during eye movements induced either in normals or by ocular motor dysfunction.

Upon initial inspection, it might appear that by adding the ‘missing’ pieces to the saccades’ duration (e.g., Figure 5), we have made them too long; the position-derived saccade duration looks like a better fit in some subjects. However, examination of skewness properties suggests that the velocity-derived timing is correct. (In the RSR responses, saccadic durations also were increased for saccades both with and against the pursuit, a strong argument for the exclusive use of velocity points to determine timing.) When the peak-velocity correction is also included, some CN subjects who did not previously appear to have normal characteristics now fit the standard relationships. Bahill et al. [46] concluded that duration was not as reliable a metric as previously stated. By comparison, normals seemed more stereotyped from subject to subject in duration than CN subjects. This is a good illustration of the variability inherent in biological systems, especially when the system is perturbed from its nominal operating range.

Using the velocity-derived duration in the calculation of skewness yielded better results for both the PC and  $PP_{fs}$  waveforms. However, the improvement for one subject’s (S5)  $PP_{fs}$  braking saccades (not shown) were not as noticeable, merely shifting the points towards the expected range rather than into it, whereas

the foveating saccade improvements were more obvious, shifting most of the saccades into the expected range. As noted earlier, the smaller a saccade, the more likely it is to be affected by the interaction with the slow-phase velocity. In this case, the slow phase just before the onset of either the braking or foveating saccades is essentially the same, but since foveating saccades are larger, they suffer less from the admixture, and therefore show more ‘normal’ characteristics when examined. This is supported by the data shown for S8, for these braking saccades are larger still, and show excellent fit to the expected range.

The broader skewness distributions for CN-related saccades versus normal saccades, while still fitting well in the defined normal range, may reflect an artifact of the method used to determine saccadic endpoints. More probably, it reflects the higher degree of difficulty in programming the former than the latter. That is, the CN slow phases were accelerating, whereas the smooth pursuit velocities were constant. A similar effect was seen to a lesser degree in the RSR responses of the normal subjects (i.e., saccades with and without pursuit).

As the models demonstrated, the simple linear, mechanical interaction between the saccade and the initial velocity is enough to significantly truncate the magnitude of the braking saccade. The presence of this mechanical interaction does not rule out the possible existence of further interaction at a more central neural level (e.g., cancellation of motor commands), or of non-linear effects (either secondary, or even the primary interaction which we have modelled as linear), but such mechanisms do not appear to be necessary to explain the largest deviations from the norm for braking-saccade characteristics. In fact, our model results suggest that such additional mechanisms may be present; perhaps this is due to slow-phase/fast-phase interactions as mentioned by Zee et al. [44]. Determination of saccade durations using the model confirmed that the velocity-criteria method (perhaps in combination with acceleration and/or jerk) is a more accurate way to determine duration.

The two-pole, one-zero model’s increased response to the slow-phase/saccade interaction was due to its plant’s greater sensitivity to stimuli, a consequence of the inertia-reducing zero. We have included the results of both models to demonstrate that the cancellation/potential effect is not limited to the more ‘realistic’ two-pole, one-zero plant, but is also present in the simpler two-pole plant. The latter is perfectly adequate for use in modeling that does not

require exact simulation of initial trajectory dynamics, but is more concerned with later dynamics and the steady-state response.

Note that the greatest effect on saccade magnitude occurred for the smaller saccades (under  $5^\circ$ ) which is also the range for most braking saccades. For larger saccades the effect is still noticeable, although apparent only at higher velocities. This suggests that larger foveating and refixation saccades (such as those in jerk and jerk with extended foveation waveforms) are probably also affected to a lesser degree, perhaps not enough to be obviously noticeable except in the most intense CN waveforms.

There have been other studies that included small saccades (i.e., saccades under  $1^\circ$ ) [1, 47–49]. In general, our data compare favorably with those of Kapoula et al. and Abadi et al., who both published peak-velocity values that fit standard relationships well (although neither examined duration). The smallest saccade ( $<5^\circ$ ) data of Smit et al. [16] overlap the relevant portions of the Boghen and Becker curves, as well as ours. Abadi and Worfolk [28] found a statistically significant reduction in peak velocities for CN subjects versus normal subjects. However, their methods do not mention how peak velocities were calculated, so it is possible that the small differences between the two groups could be due to a failure to account for the slow-phase velocity just before the saccade. Furthermore, their data fall on or near Becker and the high Boghen curves, well within normal variation. Finally, their statistical method may not have been sufficient for the analyses required; i.e., they applied the Student's *t*-test to each amplitude-cluster of data. The multiple *t*-tests may capitalize on the chance event of finding a significant effect. An analysis of the regression lines or an analysis of variance followed by a *post-hoc* test, such as Bonferroni, would have been better choices to support the contention of differences.

Too strong a dependence on the strict interpretation of saccadic velocity- and duration-amplitude relationships can lead to the discovery of problems where none actually exist. Although, at first glance, braking saccades do not always fit these standard relationships, a deeper examination of their properties suggests that they are not pathological, but are normal, non-visually triggered, fast-phase eye movements whose magnitudes have been diminished by their opposition to the runaway slow phases that characterize CN. Therefore they would seem to be closer to visually evoked saccades, rather than other types of non-visually elicited saccades, such as anti-saccades,

saccades made in the dark or to remembered targets or to auditory positions, as these demonstrate differences likely due to more complex processing.

While it may be possible to find a more complex non-linear method to 'correct' braking saccade magnitudes, i.e., attempt to elicit their original pre-programmed values, the effort to do so seems unnecessary, given the strong evidence supporting the hypothesis that braking saccades are generated by the same mechanisms responsible for voluntary and foveating saccades.

### Acknowledgements

This work was supported in part by the Office of Research and Development, Medical Research Service, Department of Veterans Affairs. Preliminary work was presented in part at the 1997 NANOS and ARVO meetings. We gratefully acknowledge the assistance of Cleve Gilmore for his incisive comments on statistical methods.

### References

1. Zuber BL, Stark L. Microsaccades and the velocity-amplitude relationship for saccadic eye movements. *Science* 1965; 150: 1459–60.
2. Yarbus AL. *Eye movements and vision*. New York: Plenum Press, 1967: 129–40.
3. Boghen D, Troost BT, Daroff RB, Dell'Osso LF, Birkett JE. Velocity characteristics of normal human saccades. *Invest Ophthalmol* 1974; 13: 619–23.
4. Bahill AT, Clark MR, Stark L. The main sequence: A tool for studying human eye movements. *Math Biosci* 1975; 24: 191–204.
5. Abel LA, Hertle RW. Effects of psychoactive drugs on ocular motor behavior. In: Johnston CW, Pirozzolo FJ, eds. *Neuropsychology of eye movements*. Hillsdale: Lawrence Erlbaum Associates, 1988: 83–114.
6. Zee DS, Optican LM, Cook JD, Robinson DA, Engel WK. Slow saccades in spinocerebellar degeneration. *Arch Neurol* 1976; 33: 243–51.
7. Abel LA, Dell'Osso LF. Correlations between saccadic latency and velocity in neurologic patients and elderly, but not young, normal subjects [ARVO abstract]. *Invest Ophthalmol Vis Sci* 1988; 29: 347.
8. Sharpe JA, Zackon DH. Senescent saccades. *Acta Otolaryngol (Stockholm)* 1987; 104: 422–8.
9. Hainline L. Normal lifespan developmental changes in saccadic and pursuit eye movements. In: Johnston CW, Pirozzolo FJ, eds. *Neuropsychology of eye movements*. Hillsdale: Lawrence Erlbaum Associates, 1988: 31–64.
10. Schmidt D, Dell'Osso LF, Abel LA, Daroff RB. Myasthenia gravis: Dynamic changes in saccadic waveform, gain and velocity. *Exp Neurol* 1980; 68: 365–77.

11. Schmidt D, Dell'Osso LF, Abel LA, Daroff RB. Myasthenia gravis: Saccadic eye movement waveforms. *Exp Neurol* 1980; 68: 346–64.
12. Wirtschafter JD, Weingarden AS. Neurophysiology and central pathways in oculomotor control: Physiology and anatomy of saccadic and pursuit movements. In: Johnston CW, Pirozzolo FJ, eds. *Neuropsychology of Eye Movements*. Hillsdale: Lawrence Erlbaum Associates, 1988: 5–30.
13. Sharpe JA, Troost BT, Dell'Osso LF, Daroff RB. Comparative velocities of different types of fast eye movements in man. *Invest Ophthalmol* 1975; 14: 689–92.
14. Smit AC, Van Gisbergen JAM, Cools AR. Dynamics of saccadic tracking responses: Effects of task complexity. In: O'Reagan JK, Levy-Schoen A, eds. *Eye Movements: From physiology to cognition*. North Holland: Elsevier Science Publishers BV, 1987: 7–16.
15. Whittaker SG, Cummings RW. Foveating saccades. *Vision Res* 1990; 30: 1363–6.
16. Smit AC, Van Gisbergen JAM, Cools AR. A parametric analysis of human saccades in different experimental paradigms. *Vision Res* 1987; 27: 1745–62.
17. Kenyon EC, Ciuffreda KJ, Stark L. Unequal saccades during vergence. *Am J Optom Physiol Optics* 1980; 57: 586–94.
18. Jacobs JB, Erchul DM, Dell'Osso LF. Braking saccade generation in congenital nystagmus. *ARVO abstracts. Invest Ophthalmol Vis Sci* 1996; 37: S277.
19. Jacobs JB, Dell'Osso LF, Erchul DM. Generation of braking saccades in congenital nystagmus. *Neuro-Ophthalmology* 1999; 21: 83–95.
20. Dell'Osso LF, Daroff RB. Braking saccade – A new fast eye movement. *Aviat Space Environ Med* 1976; 47: 435–7.
21. Dell'Osso LF, Gauthier G, Liberman G, Stark L. Eye movement recordings as a diagnostic tool in a case of congenital nystagmus. *Am J Optom Arch Am Acad Optom* 1972; 49: 3–13.
22. Dell'Osso LF, Averbuch-Heller L, Leigh RJ. Oscillopsia suppression and foveation-period variation in congenital, latent, and acquired nystagmus. *Neuro-Ophthalmology* 1997; 18: 163–83.
23. Jacobs JB, Dell'Osso LF. A model of congenital nystagmus (CN) incorporating braking and foveating saccades. *ARVO abstracts. Invest Ophthalmol Vis Sci* 2000; 41: S701.
24. Jacobs JB. An Ocular Motor System Model that Simulates Congenital Nystagmus, Including Braking and Foveating Saccades. (Ph.D. Dissertation). In: *Biomedical Engineering*. Case Western Reserve University: Cleveland, 2001: 1–357.
25. Worfolk R, Abadi RV. Quick phase programming and saccadic re-orientation in congenital nystagmus. *Vision Res* 1991; 31: 1819–30.
26. Dell'Osso LF, Daroff RB. Congenital nystagmus waveforms and foveation strategy. *Doc Ophthalmol* 1975; 39: 155–82.
27. Jacobs JB, Dell'Osso LF. Congenital nystagmus braking saccade characteristics [ARVO abstracts]. *Invest Ophthalmol Vis Sci* 1997; 38: S650.
28. Abadi RV, Worfolk R. Retinal slip velocities in congenital nystagmus. *Vision Res* 1989; 29: 195–205.
29. Broomhead DS, Clement RA, Muldoon MR, Whittle JP, Scallan C, Abadi RV. Modelling of congenital nystagmus waveforms produced by saccadic system abnormalities. *Biol Cyber* 2000; 82: 391–9.
30. Dell'Osso LF, Jacobs JB. An expanded nystagmus acuity function: intra- and intersubject prediction of best-corrected visual acuity. *Doc Ophthalmol* 2002; 104: 249–76.
31. Steinman RM, Collewijn H. Binocular retinal image motion during active head rotation. *Vision Res* 1980; 20: 415–29.
32. van der Geest JN, Frens MA. Recording eye movements with video-oculography and scleral search coils: a direct comparison of two methods. *J Neurosci Methods* 2002; 114(2): 185–95.
33. Frens MA, van der Geest JN. Scleral search coils influence saccade dynamics. *J Neurophysiol* 2002; 88: 676–91.
34. Sheth NV, Dell'Osso LF, Leigh RJ, Van Doren CL, Peckham HP. The effects of afferent stimulation on congenital nystagmus foveation periods. *Vision Res* 1995; 35: 2371–82.
35. Dell'Osso LF, Hertle RW, Williams RW, Jacobs JB. A new surgery for congenital nystagmus: effects of tenotomy on an achiasmatic canine and the role of extraocular proprioception. *J Am Assoc Pediatr Ophthalmol Strab* 1999; 3: 166–82.
36. Bahill AT, McDonald JD. Frequency limitations and optimal step size for the two-point central difference derivative algorithm with applications to human eye movement data. *IEEE Trans Biomed Eng* 1983; 30(3): 191–4.
37. Jantti V, Pyykko I, Juhola M, Ignatius J, Hansson GA, Henriksson NG. Effect of filtering in the computer analysis of saccades. *Acta Otolaryngol Suppl* 1984; 406: 231–4.
38. Enderle JD, Hallowell MB. Saccade derivative filters and their clinical implications. *Biomed Sci Instrum* 1997; 34: 206–11.
39. Winters JM, Nam MH, Stark LW. Modeling dynamical interactions between fast and slow movements: Fast saccadic eye movement behavior in the presence of the slower VOR. *Math Biosci* 1984; 68: 159–85.
40. Van Opstal AJ, Van Gisbergen JAM. Skewness of saccadic velocity profiles: A unifying parameter for normal and slow saccades. *Vision Res* 1987; 27: 731–45.
41. Collewijn H, Erkelens CJ, Steinman RM. Binocular coordination of human horizontal saccadic eye movements. *J Physiol* 1988; 404: 157–82.
42. Jacobs JB, Dell'Osso LF. A dual-mode model of latent nystagmus. *ARVO abstracts. Invest Ophthalmol Vis Sci* 1999; 40: S962.
43. Dell'Osso LF, Jacobs JB. A normal ocular motor system model that simulates the dual-mode fast phases of latent/manifest latent nystagmus. *Biol Cyber* 2001; 85: 459–71.
44. Zee DS, Fitzgibbon EJ, Optican LM. Saccade-vergence interactions in humans. *J Neurophysiol* 1992; 68: 1624–41.
45. Becker W. Metrics. In: Wurtz RM, Goldberg ME, eds. *The neurobiology of saccadic eye movements*. Amsterdam: Elsevier Science Publishers BV, 1989: 13–67.
46. Bahill AT, Brockenbrough A, Troost BT. Variability and development of a normative database for saccadic eye movements. *Invest Ophthalmol Vis Sci* 1981; 21: 116–25.
47. Steinman RM, Haddad GM, Skavenski AA, Wyman D. Miniature eye movement. *Science* 1973; 181: 810–9.
48. Kapoula ZA, Robinson DA, Hain TC. Motion of the eye immediately after a saccade. *Exp Brain Res* 1986; 61: 386–94.
49. Abadi RV, Scallan CJ, Clement RA. The characteristics of dynamic overshoots in square-wave jerks, and in congenital and manifest latent nystagmus. *Vision Res* 2000; 40: 2813–29.

*Address for correspondence:* L.F. Dell'Osso, Ocular Motor Neurophysiology Laboratory, Veterans Affairs Medical Center (127A), 10701 East Boulevard, Cleveland, OH 44106, USA  
Phone: +1-216-421-3224; Fax: +1-216-231-3461;  
E-mail: lfd@po.cwru.edu